

Chaos in a quantum well in tilted fields: A scaling system

T. S. Monteiro and P. A. Dando

*Department of Physics and Astronomy, University College, University of London, Gower Street,
London WC1E 6BT, United Kingdom*

(Received 1 June 1995)

Recent experiments have shown that the resonant tunneling diode in a tilted magnetic field is a new and promising probe of quantum chaos. We show that by using a scaling transformation a quantum spectrum is obtained that corresponds to a single classical regime and may be reliably analyzed in terms of periodic orbits. We show that for parameters close to experimental values (with an injection energy of about 25% of that due to the voltage drop), with increasing tilt angle, the disappearance of one set of fluctuations in the tunneling current is associated with a confluence where two periodic orbits are absorbed, persisting briefly in the spectrum as a “ghost.”

PACS number(s): 05.45.+b, 73.20.Dx, 73.40.Kp

Recent experimental and theoretical studies [1–3] have considered the resonant tunneling diode in a tilted magnetic field as a new example of quantum chaos. The classical dynamics of the system undergo a transition from integrable to fully chaotic as the angle between the electric and magnetic fields is varied from $\theta = 0^\circ$ to $\theta \simeq 20^\circ$. The measured tunneling current was found to be modulated by oscillations that were related to unstable periodic orbits in the chaotic regime [1]. This represents a new experimentally accessible probe of the behavior of a quantum system in the classically chaotic regime. A particular feature of the results was an abrupt change in the frequency of modulations at higher voltages [1].

Previous experimental and theoretical work on quantum chaos in real Hamiltonians has singled out Rydberg atoms in external fields. One reason is that atoms in fields are amenable to scaling transformations that considerably clarify the connections between the classical dynamics and the quantum spectrum [4]. In particular, one can measure or calculate a quantum spectrum corresponding to a single classical regime. Hence atoms have provided a powerful test of periodic orbit theory; recently interesting new dynamical effects such as core-scattered modulations [5] and ghosts [6] have been found in experimental and theoretical *scaled* atomic spectra. But in atomic systems one has the freedom to scale both the momentum and position coordinates. The quantum well problems on the other hand are constrained by the fixed width of the well, since it is impractical to change its dimensions for each experimental reading.

The resonant tunneling diode (RTD) problem consists of a single quantum well acted on by an electric field \mathbf{F} (related to the bias voltage V across the device) and a magnetic field, of strength B , tilted at an angle θ to $-\mathbf{F}$ in the x - z plane. As the voltage is varied the tunneling electrons scan the quantum energy level spectrum.

The dynamics of the electrons in the well effectively reduces to a two-dimensional classical Hamiltonian [1,3]:

$$H = E = \frac{1}{2m}(p_x^2 + p_z^2) + \frac{B^2}{2m}(x \sin \theta - z \cos \theta)^2 - eFx. \quad (1)$$

The quantum well walls are at $x = 0$ and $x = L$; $m = 0.067m_e$. The Hamiltonian is independent of y hence p_y is a constant, though $p_y \neq mv_y$. Recently [3] it was shown that in the limit where the initial kinetic energy is negligible, $E \ll V$, the classical dynamics depends only on a single parameter $\beta \propto B/V^{1/2}$. A similar property was found for a high energy limit $E \gg V$. However, this approximation does not hold in the case where E is of the same order of magnitude as V , a regime covering much of the experimental range.

Here we show that by a simple rescaling of time one obtains an exact scaling, for a given well and tilt angle, with no restrictions on the regime of validity. Further it is then possible to calculate and experimentally measure a quantum spectrum corresponding to a single classical regime. We then show that very detailed information concerning the classical motion is readily extracted directly from the quantum spectrum. We employ the substitution $\tilde{t} = tB$. In effect, $\tilde{p} = p/B$ and $\tilde{r} = r$. Then, classically, we have

$$\mathcal{E} = \frac{1}{2m}(\tilde{p}_x^2 + \tilde{p}_z^2) + \frac{1}{2m}(\tilde{x} \sin \theta - \tilde{z} \cos \theta)^2 - \epsilon \tilde{x}. \quad (2)$$

The dynamics now depends only on two parameters (other than tilt angle): a scaled energy and a scaled field \mathcal{E} and ϵ , rather than on three separate parameters E , F , and B . Crucially though, we can solve for the eigenvalues of a “rearranged” Schrödinger equation for fixed \mathcal{E} and ϵ :

$$\left(\frac{1}{2m^*}(x \sin \theta - z \cos \theta)^2 - \epsilon x - \mathcal{E} \right) \psi = \frac{B_i^{-2}}{2m^*} \nabla^2 \psi, \quad (3)$$

($m^* = 0.067$; below we use atomic units throughout) to obtain a set of eigenvalues B_i^{-2} for a set of magnetic field strengths (and the equivalent set of quantum energies $E_i = \mathcal{E} B_i^2$) corresponding to a fixed scaled energy and a fixed scaled field.

Provided the magnetic field is tunable, experiments with fixed-scaled energy and fields should then be possible. The approximate scaling proposed recently [3] also implies that the transition to chaos occurs along curves of constant $\epsilon = F/B^2$. Our proposed scaling makes clear that this holds exactly throughout, regardless of the val-

ues of field and energy. However, the classical dynamics depends in general also on scaled energy \mathcal{E} . In the experiments tuning the voltage also changes the energy of the tunneling electrons injected from the outer well. Provided the ratio of injection energy to voltage is approximately constant, then ϵ constant automatically ensures that \mathcal{E} is also constant. Then experiments at constant classical dynamics are possible for regimes of field and energy within the well. We now consider the theoretical calculations.

In periodic orbit theory [7], the quantum energy level density may be obtained (in addition to a constant term) from a sum of oscillatory contributions from each primitive periodic orbit and its multiple traversals. The frequency of these oscillations is determined by the action of the respective classical orbits and their amplitude is determined by the stability of the classical orbit. In the chaotic limit the number of periodic orbits proliferates exponentially with increasing action; hence the quantization of a chaotic system represents an infinite sum over periodic orbits. In the regular regime on the other hand [i.e., of Einstein-Brillouin-Keller (EBK) quantization] discrete quantum states may be assigned to a torus associated with one particular periodic orbit; in that case the infinite sum over multiple traversals of each periodic orbit results in a set of discrete harmonic-oscillator-like levels.

For the unscaled RTD problem the classical actions of particular trajectories and hence the frequency of the corresponding oscillation that modulates the spectrum depend on three parameters $S \equiv S(E, F, B)$ for a given tilt angle. The same applies to the stability matrix, and hence the amplitudes, of the modulations. This leads to low resolution of spectral modulations and amplitudes, which vary with spectral range. In the scaled case all eigenvalues are obtained from the same (scaled) energy and field, \mathcal{E} and ϵ . The action $S = \int pdq$; in scaled coordinates $S = B \int \tilde{p}d\tilde{q} = BS(\mathcal{E}, \epsilon)$, but $S(\mathcal{E}, \epsilon)$ is a constant, so a Fourier transform of the spectrum obtained from (3) with respect to B reveals, in the semiclassical regime, modulations of constant frequency and amplitude. The quantization condition $\int pdq = n$ in scaled coordinates becomes $\int \tilde{p}d\tilde{q} = nB^{-1}$; i.e., the n th quantum state is now associated with a different effective value of Planck's constant $\hbar = B_n^{-1}$.

We have applied the scaling technique to the experimental energy-field regime. A calculation of the actual magnitude of the Gutzwiller-type fluctuations of the tunneling current—rather than just their frequency—involves a Fourier transform of the energy-level spectrum weighted by the tunneling probability. This has not yet been done, though quantum tunneling probabilities for individual quantum states in the unscaled case have recently been calculated and a high tunneling probability was found for states visibly scarred by certain periodic orbits [2]. There it was argued that this might imply that the tunneling may be due to scarring *rather than* level clustering predicted by the Gutzwiller formula. It is not clear that one may distinguish between these effects, since the contribution of a single orbit to both scar strength as well as the energy-level density has the same

distribution as well as the same periodicity. The k th traversal of a periodic orbit contributes to the trace formula with an amplitude related to its Liapunov exponent, λ ; e.g., $1/\sinh k\lambda$ for a hyperbolic fixed point. The sum over all higher traversals in the Gutzwiller formula results in an oscillation with a Lorentzian profile of width determined by the Liapunov exponent. Where the orbit is not too unstable (i.e., the Liapunov exponent is not too large) this might be quite narrow. For a low density of states—and in [2] states where quantum numbers about 20–25 were considered—one would expect the scar strength to be concentrated mainly in a single state, since the Lorentzian encompasses few states. In the semiclassical limit where the discrete nature of the spectrum is less apparent, a proper definition of the scar strength, which detects weak scarring, will give a similar distribution to that predicted by the trace formula, as has been found in other time-independent systems with two degrees of freedom.

As yet no quantitative semiclassical theory for the tunneling current, analogous to closed-orbit theory, which has been so successful for atomic photoabsorption spectra [8], is available. This theory would provide the amplitudes for tunneling from each periodic orbit in terms of the stability parameters (the prefactors $1/\sinh k\lambda$ are valid only for the density of states) and hence allow detailed comparison between the classical dynamics and experiment. As in the atomic case, while all periodic orbits contribute to the energy-level spectrum, only a subset of the orbits is experimentally observable by means of tunneling. In the RTD case these are the orbits that cross the full length of the well from the left-hand (emitter) wall to the right-hand (collector) wall and there are further constraints from the initial energies and momenta of the tunneling electrons. But all the interesting dynamics is obtainable from the energy-level spectra, so for the moment we restrict ourselves to an analysis of the eigenvalues.

The experiments were carried out in a constant magnetic field of 11.4 T. A bias voltage of 0.4 V corresponds to an electric field $F = 2.1 \times 10^6$ V m⁻¹. In atomic units this corresponds to scaled field $\epsilon \simeq 1.75 \times 10^3$. Although ϵ , \mathcal{E} are not constant in the experiment, their ratio is approximately constant. We have estimated a value $\mathcal{E} = 600\epsilon$, in other words an injection energy equal to 26% of the voltage drop.

Figures 1(a)–1(f) show a set of classical Poincaré surfaces-of-section (SOS) taken at the collector wall, $x = L = 1200$ Å, at $\epsilon = 1.75 \times 10^3$, $\mathcal{E} = 600\epsilon$, for a set of six tilt angles $\theta = 0^\circ$ – 20° showing the transition from integrability to full chaos. The position coordinate has been transformed so that the classically allowed region is bounded by a circle of radius $\sqrt{2m^*(E + \epsilon L)}$ centered at the origin. All periodic orbits encounter the $x = L$ wall, but only a small proportion encounter the $x = 0$ wall, since few orbits have a kinetic energy component sufficient to overcome the force due to the electric field. Hence, the SOS for $x = L$ has considerably more structure (such as more islands of stability) than a corresponding SOS at $x = 0$.

Figures 2(a) and 2(b) show corresponding Fourier

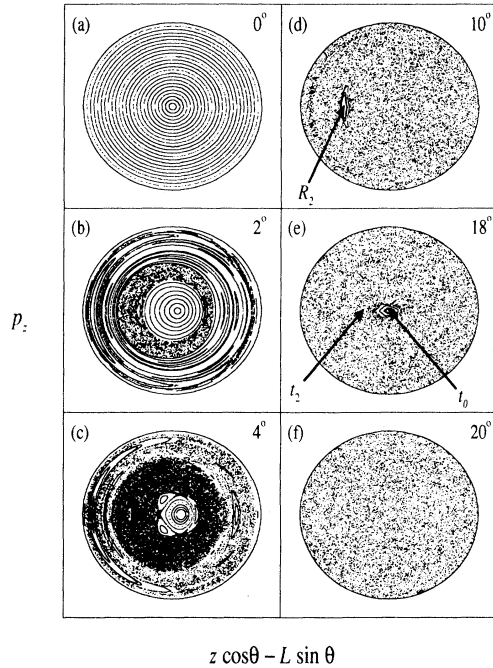


FIG. 1. Set of Poincaré surfaces of section at $x = L$ for a range of θ between $\theta = 0^\circ$ and $\theta = 20^\circ$ with $\epsilon = 1.75 \times 10^3$ and $\mathcal{E} = 600\epsilon$. The position coordinate has been transformed so that the classically allowed region is bounded by a circle of radius $\sqrt{2m^*(E + \epsilon L)}$.

transformed spectra using two sets of quantum energy levels, obtained by the solution of Eq. (3). The transforms are carried out with respect to the field-free principal quantum numbers n rather than B , since $n = \alpha B$, where $\alpha = L\sqrt{2m\mathcal{E}}/\pi$ is a constant, and span $n = 48-8$ for tilt angles $\theta = 0^\circ$ and 20° . We note that other authors sometimes refer the energy to the midpoint of the triangular well. To obtain the corresponding values of n , all our values of n given below would need to be multiplied by a factor of 1.7 and the actions should be divided by a similar factor. The system is integrable for $\theta = 0^\circ$ but fully chaotic for $\theta = 20^\circ$. Peaks of varying amplitude appear

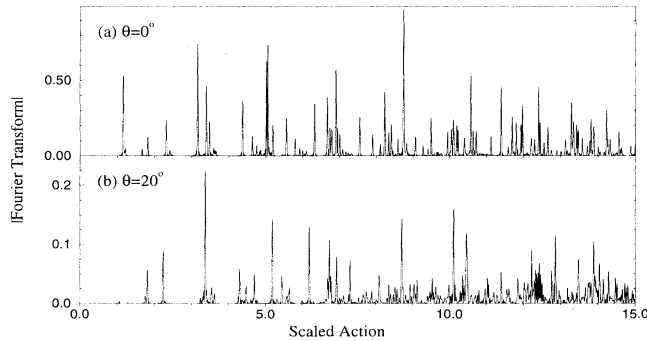


FIG. 2. Fourier transforms (*squared*) of the energy-level spectrum at $\epsilon = 1.75 \times 10^3$ and $\mathcal{E} = 600\epsilon$ for (a) $\theta = 0^\circ$ and (b) $\theta = 20^\circ$. The y axis indicates amplitudes and the x axis indicates the scaled action S in atomic units and normalized by a constant.

at positions on the horizontal axis corresponding to the classical scaled actions $S(\mathcal{E}, \epsilon)$ of the periodic orbits (the values on the horizontal axis actually correspond to S/α). The differences between Figs. 2(a) and 2(b) are very apparent for higher S , consistent with the lower amplitude or stability and the exponential proliferation of periodic orbits associated with chaotic dynamics at $\theta = 20^\circ$.

In the recent experiments, only the range equivalent to $S \lesssim 3.5$ was resolvable. With the scaling the relative contributions of the most important periodic orbits are clearly identifiable. In Fig. 3 the major periodic orbits in this range are identified for $\theta = 0^\circ$, 10° , and 20° . The computational cost of the calculation rises rapidly with θ , so for $\theta = 20^\circ$ only 2500 quantum levels in the range $n \simeq 51-10$ were used, while Figs 3(a) and 3(b) employed 4000 levels in the range $n \simeq 68-10$; hence the lower resolution in Fig. 3(c). Orbits can be assigned with confidence, since in most cases (excepting a few unresolved orbits) the position of the quantum peaks agrees with the classical scaled action to well within 0.5%. The corresponding shapes of the orbits are shown in the x - z plane in Fig. 4. The only orbits in Fig. 3 that can contribute to the tunneling are those of type t or of type S . The orbits of type R bounce only on the right-hand (collector) wall.

For $\theta = 0^\circ$ one can identify, in Fig. 3(a), eight major orbits or families of orbits that modulate the quantum spectrum. In particular, the set R_1, R_2, R_3 are periodic orbits confined to the right-hand wall, which at $\theta = 0^\circ$ have *periods* in the exact ratio 1:2:3 (the *scaled actions*, though, follow these ratios only roughly). At $\theta = 0^\circ$ there is reflection symmetry about $z = 0$ so all orbits have symmetrical pairs (e.g., R_1^+ and R_1^-). In fact, at $\theta = 0^\circ$, periodic orbits other than t_0 are not isolated, forming part of a family (a resonant torus; i.e., a torus with rational winding numbers so that the two frequencies of the motion have a rational ratio), which traces out a continuous curve in the SOS. They reduce to an isolated pair for $\theta > 0^\circ$ and the pair becomes progressively less symmetrical with increasing θ . Many orbits are subsequently born from bifurcations of such “parent” orbits (or their harmonics; $2R_1$, for example, indicates the second traversal of R_1).

There are two traversing orbits for $\theta = 0^\circ$ with resolvable periods: t_0 and t_2 , with scaled periods in the ratio 1:1.6. The periodic orbit t_0 is a straight line at $\theta = 0^\circ$ but winds about the magnetic field at higher θ . It represents the stable center of the SOS at $\theta = 0^\circ$ then loses and regains stability with increasing θ ; e.g., it is seen as the elliptic fixed point of the central island of stability at $\theta = 18^\circ$ but is unstable at $\theta = 10^\circ$ in Fig. 1. The orbit t_2 is another traversing orbit closely associated in action and is born simultaneously with R_2 . The t_3 orbits are also traversing orbits, with strong modulating amplitudes, but have double the period of t_2 .

As θ is increased the basic orbits are distorted in shape as they wind about the new magnetic field direction. For example, the shape of R_3 at 20° is shown in Fig. 4 to have tilted with the magnetic field.

A striking feature of the published experiments [1] is an abrupt doubling of the period of the fluctuations in

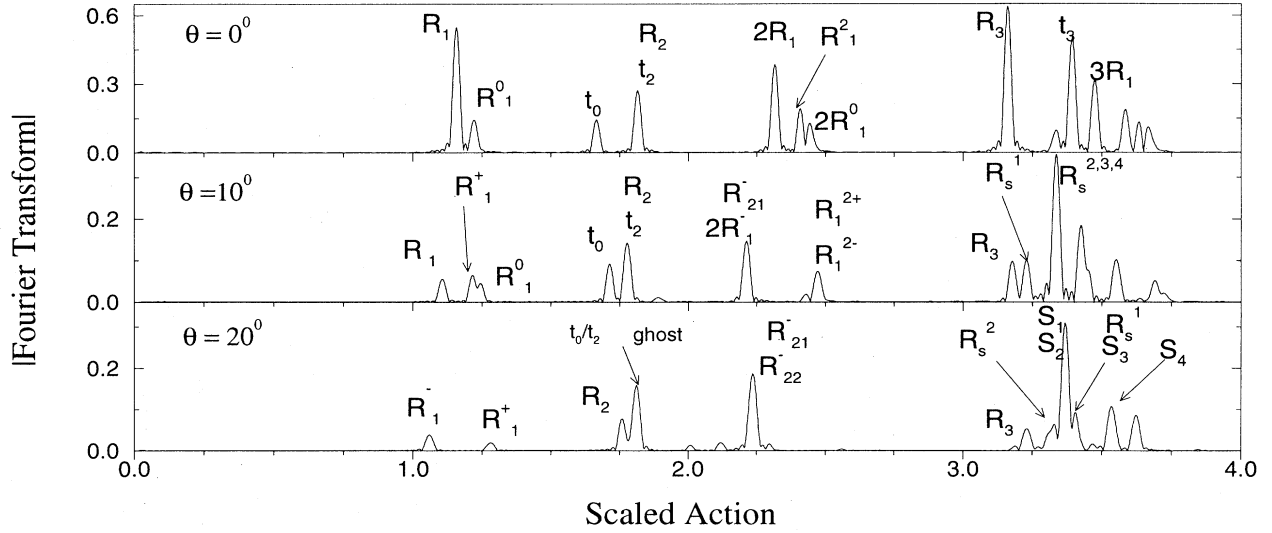


FIG. 3. Fourier transforms of the energy-level spectrum at $\epsilon = 1.75 \times 10^3$ and $\mathcal{E} = 600\epsilon$ for (a) $\theta = 0^\circ$, (b) $\theta = 10^\circ$, and (c) $\theta = 20^\circ$. Contributions from the most important periodic orbits have been identified. The same units as in Fig. 2 are used.

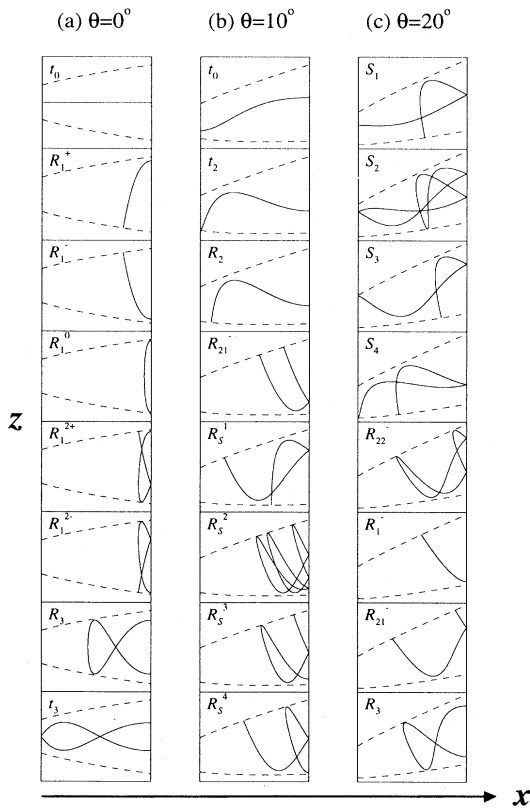


FIG. 4. Shapes of classical periodic orbits at (a) $\theta = 0^\circ$, (b) $\theta = 10^\circ$, and (c) $\theta = 20^\circ$. The broken lines indicate turning surfaces. The x axis spans the quantum well width from $x = 0$ to $x = L = 1200 \text{ \AA}$. The vertical axis represents z in the same units.

the tunneling current with increasing voltage (for $\theta = 20^\circ$ this occurred for $V \simeq 0.4 \text{ V}$). This has been shown to be consistent with a change-over in the dominant tunneling orbits from t -type orbits to new, longer period “ S ” orbits [1] that bounce twice on the collector wall and once on the emitter wall before closing.

We now use the method to consider how the variation of the classical dynamics with θ manifests itself in the spectra. In Figs. 3(a) and 3(b) we see that at $\theta = 0^\circ$ and $\theta = 10^\circ$ the quantum peaks associated with t_0 and t_2 are distinct, though close in action. But on the SOS the fixed points corresponding to t_0 and t_2 gradually approach each other as θ is increased. At $\theta = 18^\circ$, t_0 corresponds to an elliptic fixed point, marked on the SOS, at the center of the last stable island, and t_2 to a hyperbolic fixed point close by. Here these orbits both exist in a region of phase space accessible to the tunneling electrons, so they might be expected to contribute to the observed current. As the island shrinks, the two fixed points approach and eventually coalesce, annihilating each other at θ just below 20° in a confluence, the inverse of a saddle-node bifurcation and where two fixed points vanish. At nearby values of ϵ the same process occurs at a slightly different angle.

The quantum spectrum for $\theta = 20^\circ$, Fig. 3(c), shows that the peaks have coalesced into a single peak at $S = 1.81$. This is a “ghost,” since it appears above the saddle-node bifurcation, in other words, where the classical orbits no longer exist. The height of this peak is sensitive to the spectral range employed. Near a bifurcation and for low n the standard semiclassical amplitude must be replaced by a new amplitude obtained using a normal form for the generating function [6]. The amplitude of the “ghost” falls off rapidly with distance from the bifurcation (i.e., increasing θ) and our calculations

show that for $\theta > 25^\circ$ the ghost's amplitude is negligible.

It is worth stressing that the confluence occurs for the injection energies we considered here—of about one quarter of the voltage drop across the well. For lower injection energies the t_0 orbit's fixed point moves to the edge of the SOS and the orbit no longer has sufficient kinetic energy to reach the left-hand side. This is a different dynamical situation from the disappearance of the fixed point within the SOS: here nearby trajectories can still bounce alternately between walls, but fail to close to form periodic orbits. When the tunneling due to the t orbits is small, the tunneling becomes dominated by a set of four orbits S_1, S_2, S_3, S_4 in which the electrons bounce twice on the collector wall before returning to the emitter wall. They all have significant amplitude in Fig. 3(c) but in particular S_1 and S_2 form a peak of large amplitude at an action $\simeq 3.37$. They have periods about twice those of the t orbits at $\theta = 20^\circ$. These two orbits are born together just below $\theta = 13^\circ$ and their actions remain close (they are unrelated to the t orbits). In the (unscaled) experiments, the oscillations due to these orbits are only resolvable at voltages greater than 0.4 V. Figure 3(c) corresponds to a regime where the periods of S_1 and S_2 , respectively, both have periods within the experimental resolution limit of 0.63 ps [1].

In conclusion, we have shown that by using a rescaled

time we may generate a quantum spectrum corresponding to a *single* classical phase-space regime, although we have restricted ourselves to the case where the effective mass is constant. Any voltage dependence of the effective mass in the experiment, e.g., $m = m_0 f(V)$, may easily be incorporated, though since the classical dynamics are constant if $m\epsilon$ and $m\mathcal{E}$ is constant. Hence in the experiment one might need to deviate significantly from a parabolic relationship between voltage and magnetic field in order to keep $f(V)\epsilon$ and $f(V)\mathcal{E}$ constant.

It is then relatively easy to relate the modulations of the quantum spectrum to the actions and stabilities of classical periodic orbits in the chaotic regime. Dynamical effects like ghosts are then exposed. A similar advantage would be gained in studies of effects like level statistics and scars.

Note added: New experiments [9] have demonstrated the importance of bifurcations in this system, showing that t_0 loses and regains stability with increasing field.

The authors wish to thank Dominique Delande, Mark Fromhold, and Dima Shepelyansky for helpful discussions. We especially thank D. Delande for providing his Lanczos matrix diagonalization routines. The authors both acknowledge support from the EPSRC.

-
- [1] T.M. Fromhold *et al.*, Phys. Rev. Lett. **72**, 2608 (1994).
 [2] T.M. Fromhold *et al.*, Phys. Rev. Lett. **75**, 1142 (1995).
 [3] D.L. Shepelyansky and A.D. Stone, Phys. Rev. Lett. **74**, 2098 (1995).
 [4] D. Wintgen, Phys. Rev. Lett. **58**, 1589 (1987).
 [5] P.A. Dando, T.S. Monteiro, D. Delande, and K.T. Taylor, Phys. Rev. Lett. **74**, 1099 (1995).
 [6] M. Kuś, F. Haake, and D. Delande, Phys. Rev. Lett. **71**, 2167 (1993).
 [7] M.C. Gutzwiller, *Chaos in Classical and Quantum Mechanics* (Springer-Verlag, New York, 1990).
 [8] M.L. Du and J.B. Delos, Phys. Rev. A **38**, 1913 (1988); J. Gao and J.B. Delos, *ibid.* **46**, 1455 (1992).
 [9] G. Muller, G.S. Boebinger, H. Mathur, L.N. Pfeiffer, and K.W. West, Phys. Rev. Lett. **75**, 2875 (1995).